LA-UR-20-27525
Approved for public release; distribution is unlimited.

Title: Validation of Reactive Flow Capabilities in PAGOSA

Author(s): Culp, David Benjamin
Aslam, Tariq Dennis

Intended for: Report

Issued: 2020-09-24

Validation of Reactive Flow Capabilities in PAGOSA

David Culp, XCP-2
Tariq D. Aslam, T-1
Los Alamos National Laboratory, Los Alamos, NM 87545

September 17, 2020

Abstract

Several reactive flow modeling capabilities are studied and applied to physics problems of interest in the PAGOSA hydrocode with an emphasis on validation. The Davis equation of state and the Arrhenius shock temperature dependent WSD (AWSD) reactive flow model have been implemented by the author in PAGOSA over the last year. These high-explosive modeling options along with the previously existing HE-JWL equation of state and the SURF/SURFplus reactive flow models are discussed, exercised and compared. Validation of the models analyze numerical results against experimental data from cylinder tests, two-stage gas gun experiments and proton radiography (pRad) experiments. Applications of the modeling options are explored involving both HMX based PBX 9501 and TATB based PBX 9502. The effect of mesh size is considered for prediction of phenomena such as corner turning and dead zones, and the relative code performance of the modeling options is discussed.

---

1 Introduction

Reactive flow modeling is paramount to many PAGOSA users and provide key physics capabilities when studying the behaviors of high explosives. The combination of a reactant equation of state (EOS), product EOS, a mixture model and an HE reactive burn model allow for run time calculations that dictate the demeanor of the HE reaction. The calculation of pressures and temperatures of the HE by the EOS are connected to the burn fraction (λ), or progress variable, rate calculation via a two-way coupling. Some of the more cutting edge tools consist of the HE-JWL and Davis equations of state used in conjunction with the SURF/SURFplus and AWSD reactive burn models [1, 2, 3]. Of these, Davis and AWSD have only recently been implemented in PAGOSA. Until this time, there has been very little validation of these tools, therefore the scope of this report will focus on doing so for combinations of the aforementioned modeling options.

Additionally, this work aims to demonstrate the capabilities of these tools. These include their ability to accurately model the shock to detonation transition, predict detonation velocities and resolve and predict phenomena such as dead zones and corner turning over a range of different mesh resolutions. HMX based PBX 9501 and TATB based PBX 9502 both have calibrations readily available for these modeling options and will serve as the materials of interest in these studies. Data from gas gun shots, cylinder tests and pRad experiments are compared and contrasted with results of the numerical simulations and serve as validation vehicles.

2 Description of Models

This section introduces the two equations of state and the two reactive burn models of interest in this report. It is in no way meant to be an exhaustive description, but merely an overview.

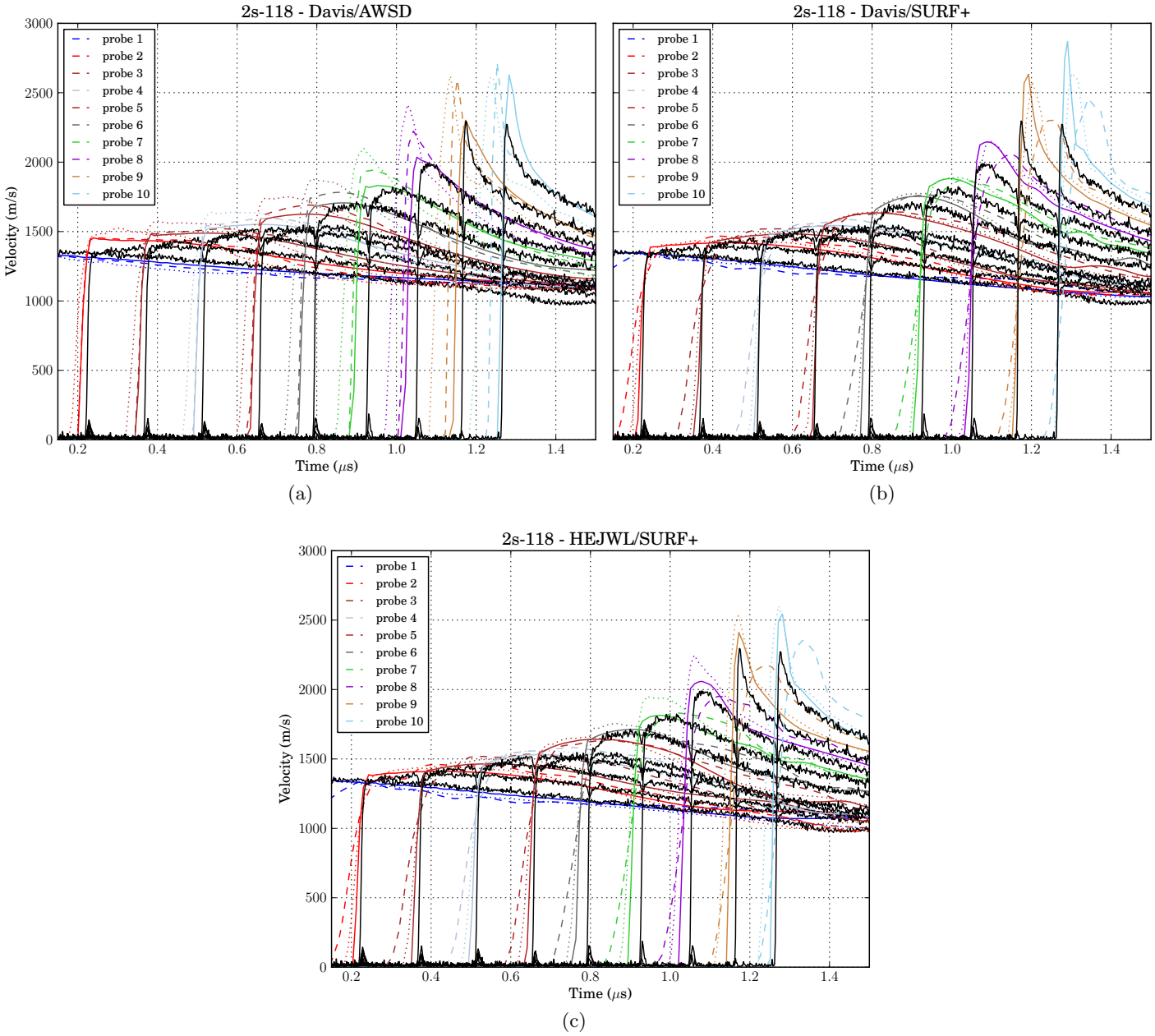

Figure 1: Simulated velocities over a range of resolutions for shot 2s-118 are compared to experimental using Davis/AWSD in (a), Davis/SURFplus in (b) and HEJWL/SURFplus in (c). Dashed lines represent 200 microns, dotted 100 microns and solid 50 microns, with the experimental data plotted in solid black.

2.1 HE-JWL Equation of State

The HE-JWL EOS has been heavily used in PAGOSA in conjunction with reactive burn models such as Multi-Shock Forest Fire (MSFF) and SURF. The parameters for PBX 9501 and 9502 and details of its implementation and use can be found in [2]. The reactant portion uses a linear U_s-U_p Mie-Grüneisen [4] form with a Walsh-Christian temperature [5]. The product portion uses a JWL [6, 7] form. When a cell is partially burned, a secant method algorithm iterates on the solid-density (ρ_s) enforcing pressure-temperature (pT) equilibrium in the mixed, or burning, cell. The converged solution of ρ_s is used to solve for the gas-density (ρ_g), which is used to calculate the pressures in the mixed cells.

HE-JWL is limited to working with burn models that do *not* require temperature as an input and for this reason is not able to be used with AWSD. In this report, it is only used in conjunction with SURF/SURFplus. By design, the EOS only iterates on mixed cells that fall in a particular density/burn fraction regime, which is dictated by user-driven tolerances. If a burning cell falls outside of this range, the iteration process is bypassed, and the pressure calculation is simply a scaling of the incoming material pressure. In general, the HE-JWL EOS performs relatively quickly for this reason, but also does not provide high-fidelity predictions in such regimes.

2.2 Davis Equation of State

The Davis EOS was recently added to PAGOSA and is considered fully functional in code versions 17.3.12 and later. Parameters for PBX 9501 and PBX 9502 are outlined in [8, 3], respectively. Using Mie-Grüneisen forms for both products and reactants, a secant-like method [9] is employed to solve for Φ, which is defined as the ratio of specific volumes: $\Phi = v_r/v_p$. The book keeping needed for the partition of reactants and products in a burning cell is handled by Φ. Closure for the mixture model is possible with enforcement of pT equilibrium.

This wide-ranging EOS has several qualities that are not realized in HE-JWL. When the secant method fails to converge on a physical solution of Φ, a bisection method algorithm hones in on a solution that is physical. While this may introduce computational expense in certain regimes, it ensures a high-fidelity temperature and pressure calculation that HE-JWL avoids. Being a complete EOS, the temperature, pressure and sound speeds are calculated for all cells of the material. This makes the EOS amenable to use with the AWSD burn model as well as other reactive burn models such as SURF/SURFplus, or MSFF. The EOS was designed to be valid over a large swath of pressures and can handle over-driven regimes.

2.3 AWSD Reactive Burn Model

The Arrhenius Wescott-Stewart-Davis (AWSD) reactive burn model is a recent adaptation of the WSD formulation [10]. This ignition and growth type model has a reaction rate calculation primarily based on the an approximation of shock temperature with Arrhenius terms. Both local pressure and the burn fraction are additionally employed to calculate the rate. Typically, the model is coupled with the Davis EOS to form a complete reactive flow model, whose full sets of parameters for PBX 9501 and PBX 9502 have been calibrated over a wide ranging thermodynamic regime. Such parameterizations for PBX 9501 and PBX 9502 are outlined in [8, 3], respectively, and are those used for all of the Davis/AWSD simulations in this report. Conceivably, the AWSD reactive burn model could be used in conjunction with some other complete EOS that calculates temperature and pressure, such as a SESAME or some analytic EOS, but such a combination has yet to be tested.

One of the more useful attributes of this model is that its temperature-based rate allows a single parameterization of a given material to handle a large range of initial thermodynamic states. For instance, a cold (T_0 =77 K at ρ_0 =1.942 g/cm^3), a nominal (T_0 =297 K at ρ_0 =1.890 g/cm^3) and a hot (T_0 =403 K at ρ_0 =1.840 g/cm^3) PBX 9502 use the same EOS and burn model parameterizations and are differentiated simply by altering the material's user-specified initial density and specific internal energy. This is not the case with other reactive burn models, such as SURF, which require additional parameterizations for different initial states.

2.4 SURF Reactive Burn Model

The SURF burn model is also founded on an ignition and growth concept whose main premise is that burn fronts are formed from activated hot spots along a shock front. Using a shock detector algorithm, SURF's rate calculation is based on the shock pressure. In TATB based explosives it is often of interest to take the additional carbon clustering into account during calculation of the reaction rate. PAGOSA's implementation of SURFplus does this by using an additional reaction progress variable and adjusting the specific internal energy accordingly.

In this report, we will use fitting forms 4 of SURF and SURFplus for modeling of PBX 9501 and PBX 9502, exclusively. More about the models forms, assumptions and their parameterizations can be found in [11, 1].

2.5 Numerical Setting

The PAGOSA hydrodynamics code is an Eulerian Volume of Fluid(VOF) finite difference solver that is capable of simulating massively parallel 2D and 3D problems. Using a staggered grid, the predictor-corrector methods are 2nd order accurate in space and time and utilize a Youngs interface reconstruction with Youngs/van Leer advection methods. Multiple options for handling material strength, HE-Burn and artificial viscosity allow for a myriad of modeling strategies. The artificial viscosity was left at its default setting for the entirety of the tests run in this report, which is the Wilkins' form using the length across the cell in the vector direction of maximum pressure gradient [12].

Because it does not support AMR, special attention is required to choose a mesh resolution that satisfies the features one needs to resolve. For large 3D runs, mesh sizes smaller than 300 microns can become unfeasible in some cases, but resolutions down to 10 microns may be reasonable for small-scale problems, especially in 2D.

3 Gas-Gun Simulations

In order to validate and explore the models' predictive one-dimensional shock-to-detonation transition (SDT) capabilities, 2-stage gas gun experiments were simulated. These small scale experiments involve using a gas gun to propel a flyer which impacts a sample of HE. Embedded gauges within the HE are a diagnostic used to produce a time history of velocities of the shock and detonation waves traveling through the HE. These validation experiments are especially useful in testing the accuracy of the reactant EOS and shock to detonation transition.

Sources of uncertainty include lot to lot variations of the HE, the accuracy of the embedded gauge locations, impactor tilt angle, impact stress and velocity measurements. It is noted in [13] that SDT times can vary by as much as $\pm$ 20%, and the impact stresses have an uncertainty of 1.7% [14].

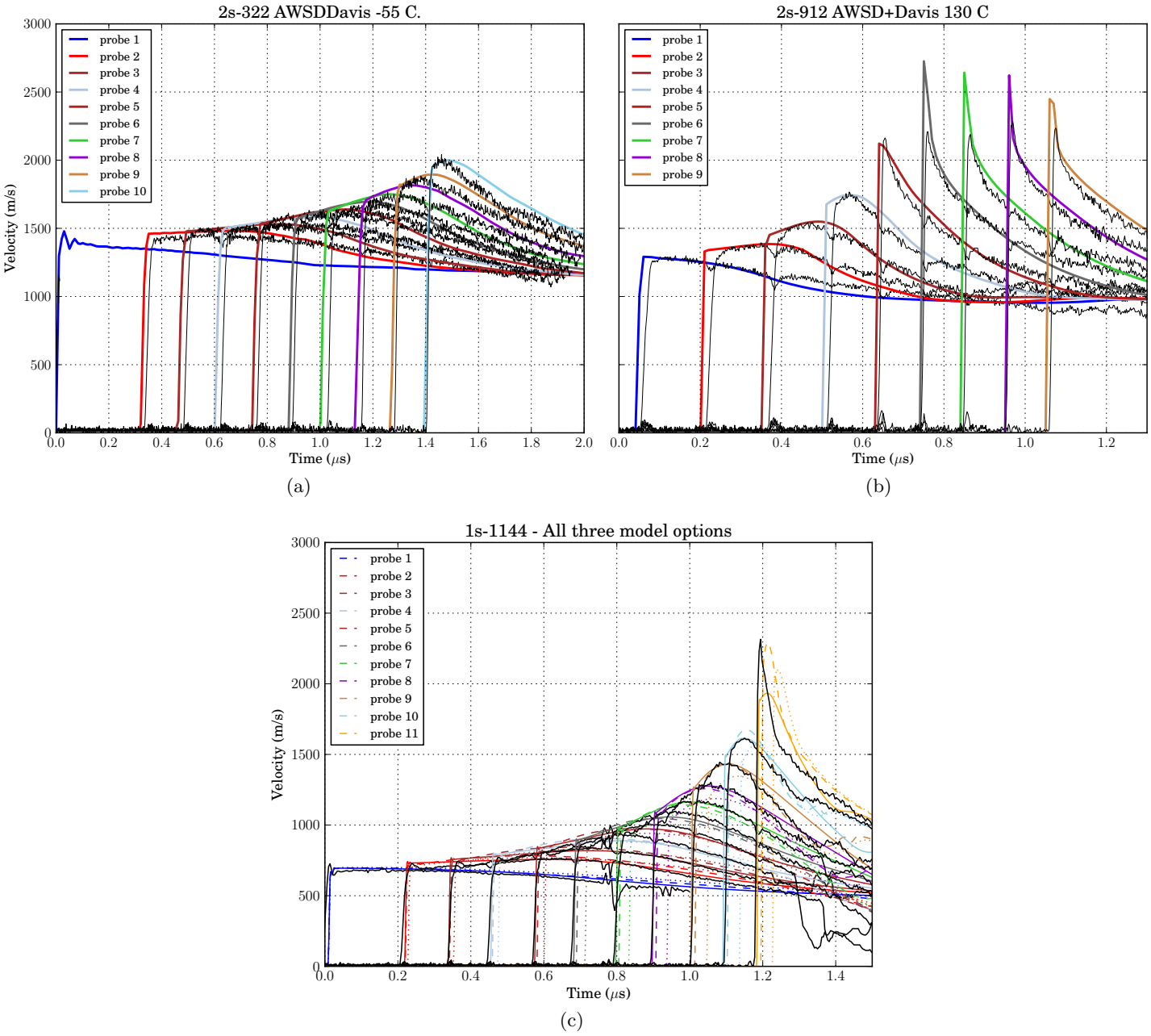

Figure 2: The velocities predicted using Davis with AWSD is compared to the experimental velocities (in black) for (a) shot 2s-322, and (b) shot 2s-912, (both 9502). Shot 1s-1144 (9501) is shown in (c), at 25 μm with Davis/AWSD as solid, Davis/SURF as dashed and HEJWL/SURF as dotted.

The following shots were simulated using a myriad of resolutions in PAGOSA, with 2D Cartesian geometry. Ten processors were employed using code version 17.3.12, in double precision. The flyer was modeled using a linear U_sU_p Mie-Grüneisen EOS. The HE was modeled using combinations of the reactive flow options described earlier. Lagrangian tracers were placed at the corresponding embedded gauge locations and serve as a diagnostic analog to the experimental embedded gauges.

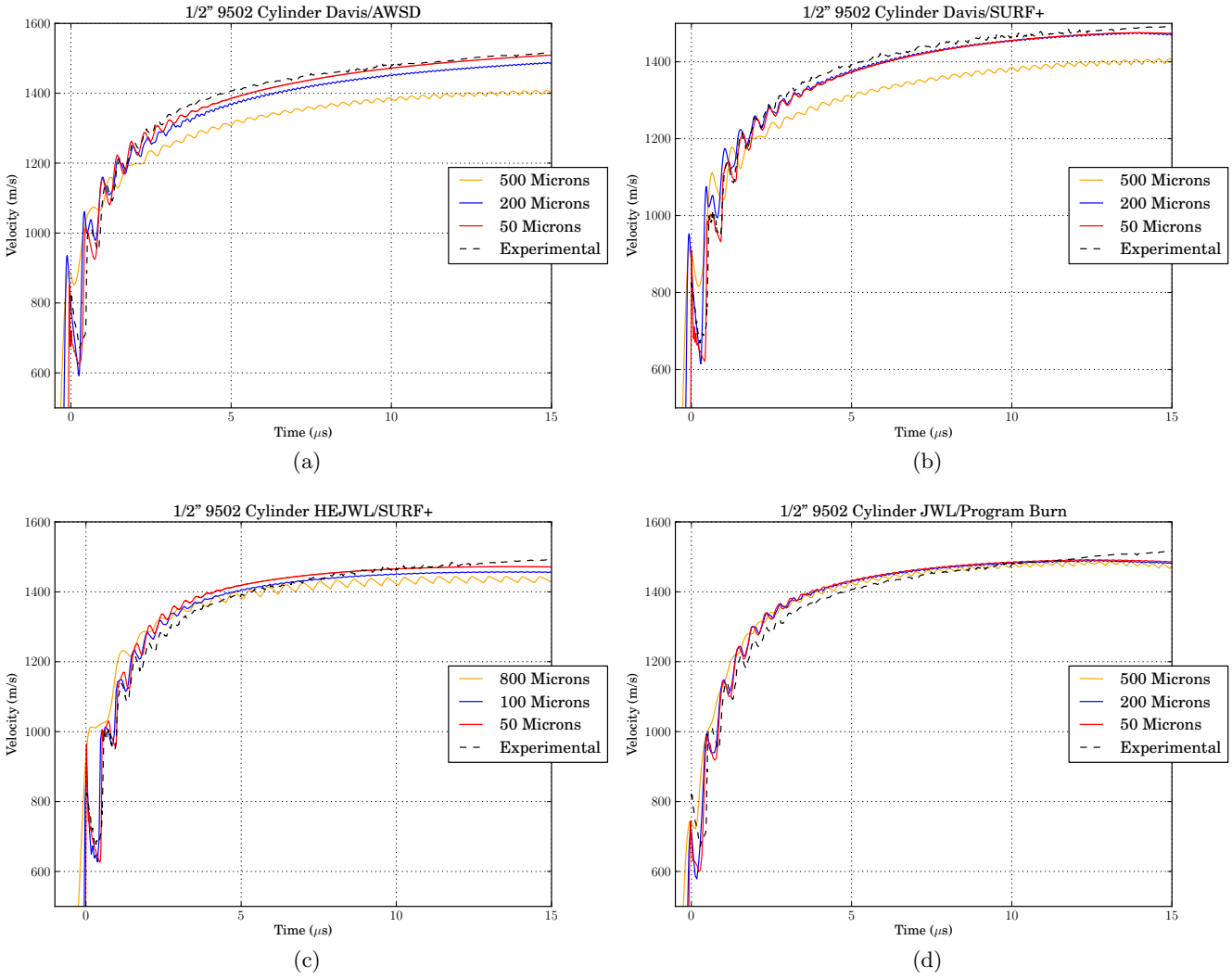

Figure 3: The PBX 9502 half-scale calculated PDV results for (a) Davis/AWSD, (b) Davis/SURFplus, (c) HEJWL/SURFplus and (d) JWL/Program burn are shown at several resolutions along with the experimental PDV (in black).

3.1 Nominal Shot

The first such experiment examined, shot 2s-118, was conducted using PBX 9502 at ambient temperatures, 23 °C. A lexan projectile with a Kel-F 81 impactor disk was fired at 2.798 km/s into a sample of PBX 9502, resulting in a 13.78 GPa impact stress. Full experimental details and results are described in [14].

The results presented in Figure 1 range from 50 μm to 200 μm. At resolutions finer than 50 μm, the results did not change significantly, and this is considered to be a converged mesh size for capturing SDT phenomena using the reactive flow options of interest. Coarser resolutions, such as 1 mm, still capture a SDT, but the timing may be off considerably, without a distinguishable SDT.

Because PAGOSA users often cannot afford to run resolutions of 200 and finer, all three of the modeling combinations were subjected to the same impact conditions as shot 2s-118 at both 1 mm and 0.5 mm mesh resolutions. All of these simulations produced a steady detonation with the 13.78

GPa up to 1 mm. Further quantifying the sensitivities of these models to impact stress and mesh resolution would be a worthwhile study with implications of modeling detonations due to fragment impact scenarios.

3.2 Hot and Cold Shots

To demonstrate the flexibility of the Davis EOS used in conjunction with the AWSD burn model, two off-nominal simulations were run and the numerical results compared with experimental data. Shot 2s-322 [15] used the exact same setup as 2s-118, except the impactor was fired at 2.820 km/s resulting in 13.75 GPa impact stress on a -55°C sample of 9502. The results are shown in 2 (a) for a 50 μm resolution. Several other resolutions were run, but 50 μm showed a converged solution.

Similarly, a hot shot is modeled with the Davis/AWSD combination. Shot 2s-912 [16], is similar to the previously described shots, but the initial velocity of the impactor was 2.522 km/s creating an impact stress of 11.6 GPa on a 130°C sample of 9502. The results are shown in 2 (b) with a 25 μm resolution compared to the experimental velocities.

3.3 Shot 1s-1144, PBX 9501 at 23°C, 5.21 GPa

It is important to show that these reactive flow capabilities are able to accurately model more than just one explosive. So far, these studies have focused on the TATB based PBX 9502. Shot 1s-1144 [17] featured a vistal impactor fired at HMX based PBX 9501 at 23°C, creating a 5.21 GPa impact stress. The shots were setup in a similar manner to those described previously, using a linear U_sU_p Mie-Grüneisen EOS for the vistal.

Results from simulations using resolutions of 10 μm are plotted for all three models and appear in part (c) of Figure 2 and shows a converged prediction of the experimental data. The PBX 9501 simulations generally will require a finer mesh since the reaction zone is shorter than that of PBX 9502.

4 Cylinder experiments

A series of exploding cylinder tests are the next experiments considered in which a cylindrical charge of HE is surrounded by a cylindrical sleeve of C101 oxygen-free copper. The charge is detonated with a PBX 9501 booster pellet adjacent to the main charge. Photon Doppler velocimetry (PDV) records the wall velocities, which is a diagnostic that is easily compared to PAGOSA's synthetic PDV. After the booster is ignited, a time history of wall velocities is captured at the PDV probes - this data can be used to construct useful quantities such as kinetic energy histories. Further, the experimental data from such tests are often used to quantify an explosive's ability to accelerate metal and may be used for fitting EOS parameters. These tests are a good way to validate the products portion of an EOS and the longer term reaction rates of a burn model as a detonation wave steadily propagates.

The PBX 9501 booster is modeled with a JWL EOS and programmed burn. The shock wave generated by this conventional HE is the mechanism that triggers the detonation of the main charge. The copper in the numerical setup employs a Sesame EOS (Table 3336) along with PTW strength to predict the metal's material response. Certain modeling choices for the copper had a large bearing on the frequencies and amplitudes of the copper's ringing and are a source of uncertainty. These periodic features are apparent in the associated figures. PAGOSA's strength_df and pmin values for the copper were two of the more sensitive parameters, and were set to 0.9 and -0.012 megabars, respectively. PAGOSA code version 17.3.12 was used with double precision to simulate

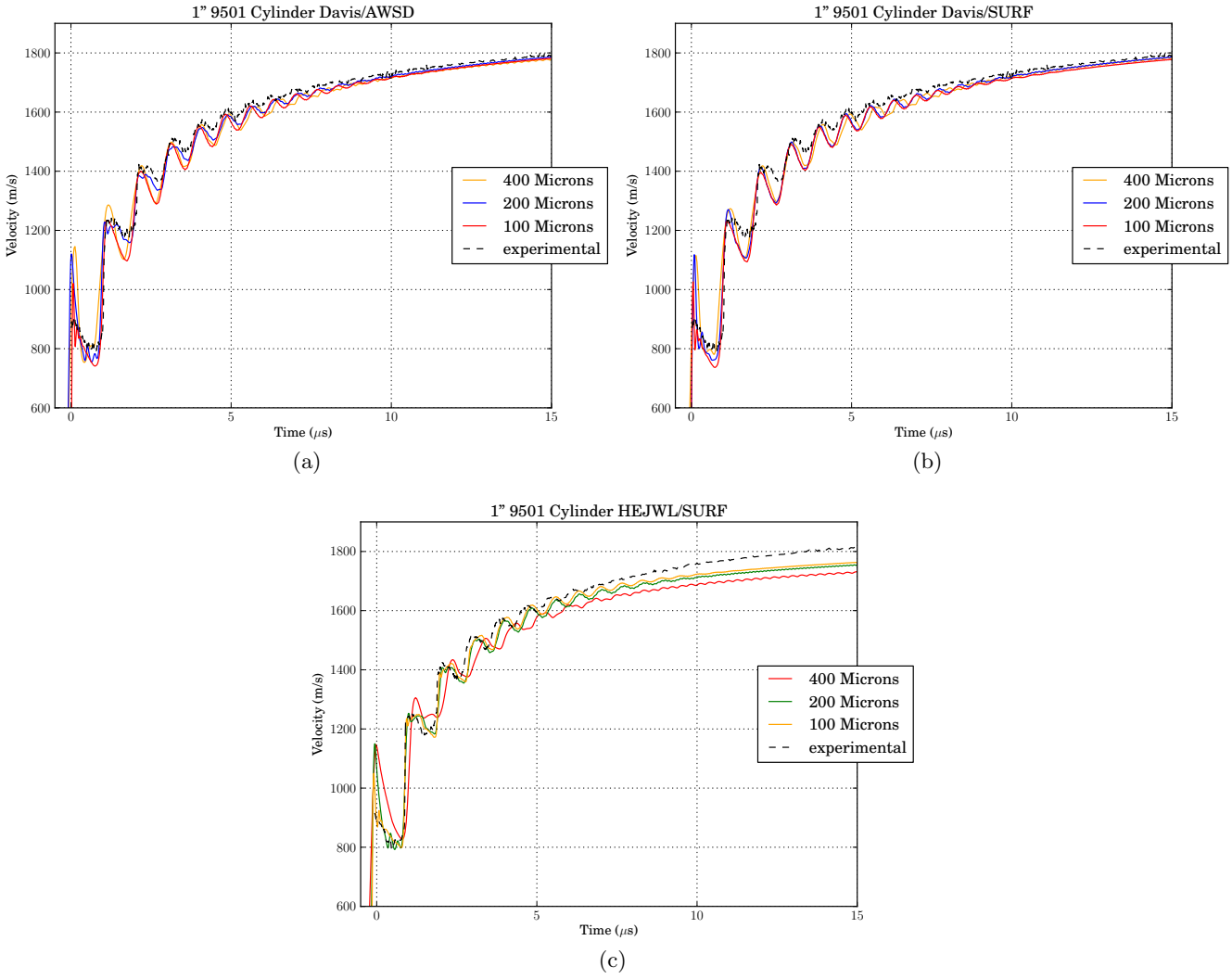

Figure 4: The 9501 full-scale cylinder numerical PDV results for (a) Davis/AWSD, (b) Davis/SURF and(c) HEJWL/SURF are plotted at several resolutions along with the experimental PDV (dashed black).

these experiments using a variety of resolutions, ranging from 1mm down to 50μm zone sizing. Because of the problem's cylindrical geometry, it was treated as an axisymmetric 2D simulation, using 240 CTS1 ranks for all of these resolutions.

4.1 Half-scale PBX 9502 Cylinder

A half-scale experiment is modeled per [18], where the copper cylinder has a length of 15.24 cm an inside diameter of 1.27 cm and a wall thickness of 0.127 cm. This is considered half-scale, as typical cylinder tests utilize cylinders twice the length and diameter. The main charge is PBX 9502 for the which the three modeling combinations of interest are used. Figure 3 shows the numerical PDV velocity time histories for four different modeling options, each at several resolutions of interest.

The measured experimental PDV data is plotted for comparison. Part (a) shows the Davis/AWSD results, with the Davis/SURFplus, HEJWL/SURFplus and JWL/reactive burn shown in parts (b),

(c) and (d) respectively. At 500 μm and finer, the velocities are predicted at well within $\pm$ 100 m/s, with a few exceptions. Worth noting, the HEJWL/SURFplus combination in 3(c) predicts later-time velocities that are within 50 m/s of those measured at a resolution of 800 μm. The program burn simulation was included in this series to compare/contrast results with the reactive burn options. This option is sufficient for prediction of velocities in a cylinder test situation, as phenomena such as corner turning and SDT are not needed with the given geometry and the use of a boosted ignition.

4.2 Full-scale PBX 9501 Cylinder

Experiment number 8-1942 fielded by Scott Jackson and Eric Anderson is a similar shot but was full-scale, with cylinder length of 30.48 cm (12 inches), main charge diameter of 2.54 cm (1 inch) and copper wall thickness of 0.254 cm. The main charge in this case is PBX 9501 and the lot was die-pressed, which can introduce significant density gradients in the material. Figure (4) presents the experimental PDV plotted against the calculated PDV for Davis/AWSD (a), Davis/SURF (b), and HEJWL/SURF (c) for various resolutions. The Davis EOS shows very accurate velocity predictions with both reactive burn models, within $\pm$ 10 m/s at even 400 μm resolutions.

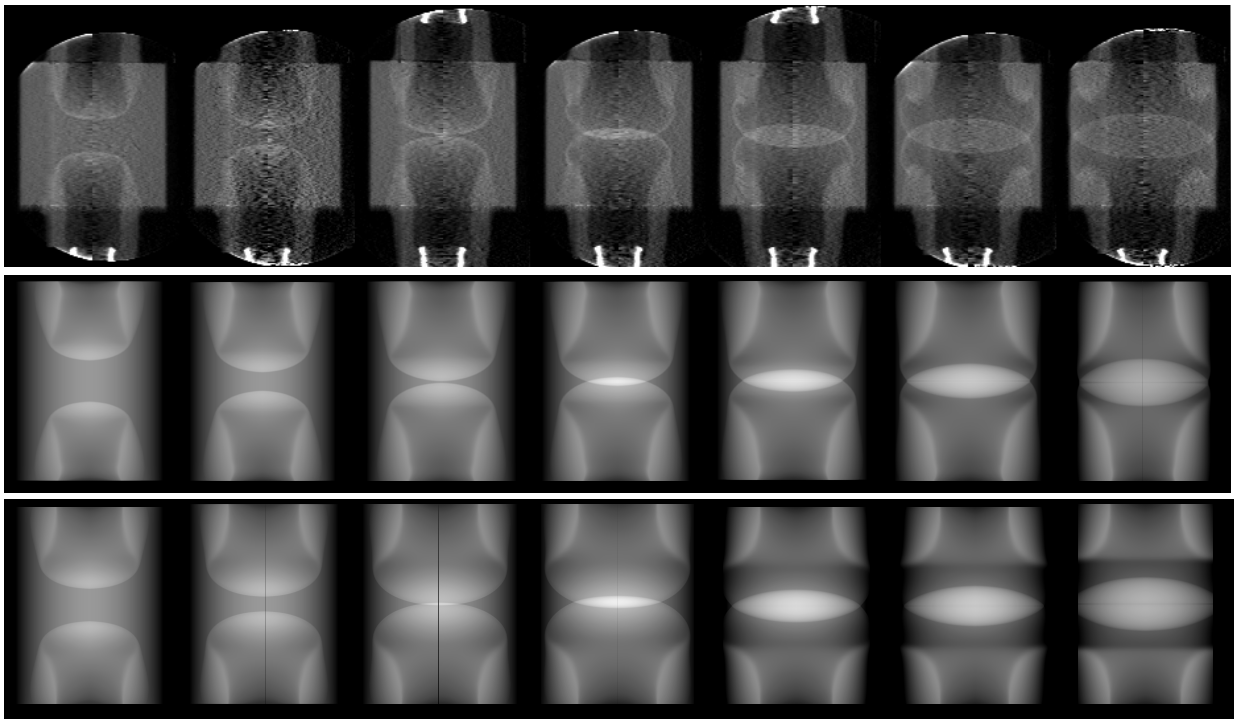

Figure 5: The experimental pRad 77 radiography from time 2.7-4.6 μs after breakout is shown on the top row. The predicted Davis/SURFplus aerial mass synthetic radiography is shown in the middle row, and Davis/AWSD on the bottom row for the same times.

5 pRad Experiments

Two of the desired predictive capabilities of reactive flow modeling are dead zone modeling and corner turning, both of which are observed phenomena in the detonation of high explosives in many

scenarios. There are a number of proton radiography experiments that capture radiography of the these processes dynamically occurring in the detonation of HE. The pRad 77 test consists of a 5cm by 5cm puck of PBX 9502 initiated from both ends with a pellet of PBX 9407. The detonation waves from both sides create an over-driven scenario as they converge in the middle of the 9502, hence this test is called the "wave-collider".

Radiography of the experiment is shown on the top row of Figure 5, and the predicted aerial mass synthetic radiography results using Davis/SURFplus and Davis/AWSD at 50 μm resolution are shown on the middle and bottom rows. The figure depicts 2.7-4.6 μs after the breakout of the PBX 9502. The white areas in the top and bottom right of each frame indicate the dead zones of the HE where there is higher aerial mass in the undetonated regions. This also demonstrates corner turning where the darker, less dense areas of detonated HE are spreading outward over time. Peak pressures of 0.963 and 1.1017 megabars were predicted with SURFPlus and AWSD, respectively, at 3.6 μs after breakout. Nearly identical results were observed with HEJWL/SURFplus and Davis/SURFplus, but AWSD predicted slightly more aggressive corner turning resulting in smaller dead zones. These differences are clear in Figure 5.

The corner turning predictions are dependent on mesh size and in the numerical experiments the behavior appeared converged when using 100 μm and finer resolutions. At 200 μm, corner turning was observed with larger dead zones predicted, while at 400 μm failure of the detonation was observed. This trend was observed across all of the models and is shown in Figure 6 for the Davis/SURFplus model.

Figure 7 shows PBX 9502's burn fractions at $t = 4\mu$s after breakout in wave collider simulations for three distinct initial thermodynamic states. This demonstrate how the HE's initial temperature affects the AWSD model's corner turning and dead zone predictions. Clearly the model predicts smaller dead zones and more aggressive corner turning behaviour with hotter HE.

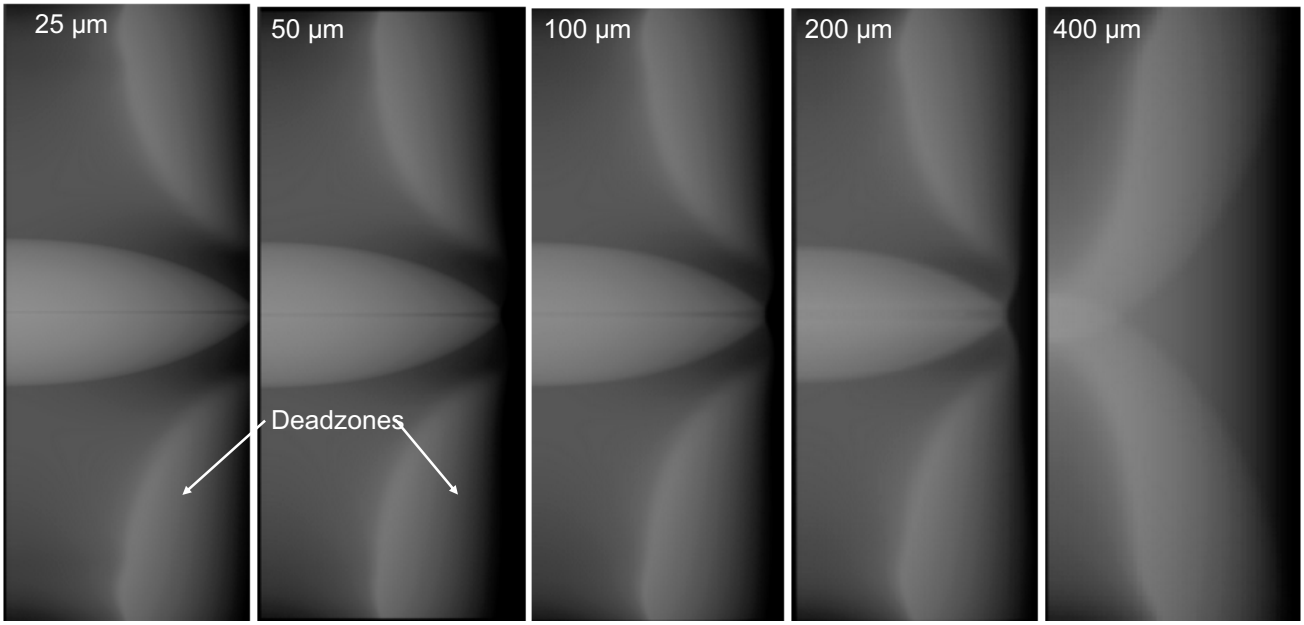

Figure 6: The areal mass density as predicted by Davis/SURFplus is shown over a variety of resolutions for the pRad 77 test. The predicted corner turning behavior and dead zone sizing appears converged at 100 microns in this scenario.

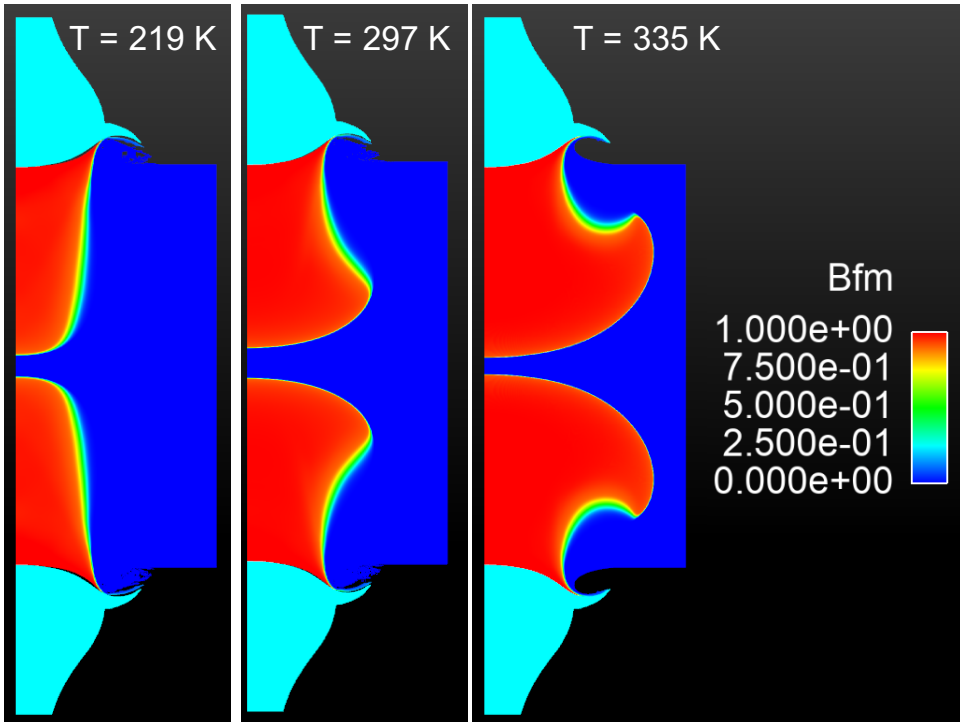

Figure 7: The burn fraction is shown plotted for three different initial HE temperatures as predicted by AWSD. The left shows no corner-turning at $T = 219$K, the center shows corner turning at ambient temperatures, while the right shows more extreme corner turning from a relatively hot HE.

6 Conclusions

These studies aimed to provide a succinct demonstration of the reactive flow capabilities in PAGOSA and validate their underlying physics. These models were shown to be useful within certain bounds, spatial resolution in particular. There are a number of other important high explosive phenomena that can be captured with these models, such as curvature effects and failure diameters, which were beyond the scope of the author's time limitations. These, and more in-depth analysis of the phenomena studied in this report, provide ripe opportunity for future validation work. Verification of the Davis and AWSD models through ZND profile tests should also be an area of future work.

The shock to detonation transition was shown to be resolved using all of the models studied, when using reasonable mesh sizing. Gas gun simulations demonstrated the ability of the reactant equations of state to capture the shock to detonation transitions in PBX 9501 and 9502. The AWSD burn model used with Davis shows flexibility in its ability to explore SDT at off-nominal temperatures by simply changing the initial thermodynamic state of the material.

The cylinder tests presented here validated the product equations of state, the reaction rates of the burn models and their ability to push metals. The experimental wall velocities showed good agreement over a range of resolutions for both of the high explosives considered. Finally, the pRad experiment showed that the models are capable of predicting dead zone sizing and corner turning at certain resolutions.

The published values of SURF and SURFplus parameters using fitting form 4 from [11, 1] presented results with the closest agreement to all of the experimental diagnostics. The same was observed with HEJWL, Davis and AWSD in [2, 8, 3] – these values are recommended for similar

numerical experiments in PAGOSA. Users of these models should carefully consider the required accuracy of the phenomena they wish to resolve when choosing a final resolution – perhaps this body of work can provide at least a starting point.

References

[1] Ralph Menikoff. SURFplus Model Calibration for PBX 9502. Technical report, 12 Los Alamos National Laboratory, LA-UR-17-31015, 2017.

[2] David Culp. The HE-JWL Equation of State in PAGOSA. Technical report, Los Alamos Scientific Laboratory, LA-CP-20-20466, 2020. Sponsor: DOE.

[3] Tariq D. Aslam. Shock temperature dependent rate law for plastic bonded explosives. *Journal of Applied Physics*, 123(14):145901, 2018.

[4] Amsden A. Harlow, F. Fluid Mechanics. Technical report, Los Alamos Scientific Laboratory, LASL-4700, 1971. Sponsor: DOE.

[5] Equation of State for Metals from Shock Wave Measurements. *Physical Review*, 97:1544, 1985.

[6] W. Weseloh. JWL in a nushell. Technical report, Los Alamos National Laboratory, LA-UR-14-24318, 2014. Sponsor: DOE.

[7] R. Menikoff. JWL equation of state. Technical report, Los Alamos National Laboratory, LA-UR-15-29536, 2015.

[8] Tariq D. Aslam, Matthew A. Price, Christopher Ticknor, Joshua D. Coe, Jeffery A. Leiding, Marvin A. Zocher. AWSD Calibration for the HMX Based Explosive PBX 9501. proceedings of the APS-SCCM conference, 2019.

[9] Tariq D. Aslam, Nirmal K. Rai, Stephen A. Andrews, Matt A. Price, and David B. Culp. On Two-Phase Pressure and Temperature Equilibration with Mie-Grüneisen Equations of State. Technical report, Los Alamos National Laboratory, in preparation for LAUR, 2020.

[10] B. L. Wescott, D. Scott Stewart, and W. C. Davis. Equation of state and reaction rate for condensed-phase explosives. *Journal of Applied Physics*, 98(5):053514, 2005.

[11] Ralph Menikoff. Verification test of the SURF model in xRage: Part IV cylindrically converging detonation wave. Technical report, Los Alamos Scientific Laboratory, LA-UR-19-26162, 2019.

[12] Wayne Weseloh and Sean Patrick Clancy. PAGOSA Input Reference Manual. Technical report, Los Alamos National Laboratory, LA-CP-17-20444, 2017.

[13] Ralph Menikoff. Review of PBX 9502 Pop Plot data. Technical report, 12 Los Alamos National Laboratory, LA-UR-18-31380, 1999.

[14] R. L. Gustavsen, S. A. Sheffield, and R. R. Alcon. Measurements of shock initiation in the tri-amino-tri-nitro-benzene based explosive pbx 9502: Wave forms from embedded gauges and comparison of four different material lots. *Journal of Applied Physics*, 99(11):114907, 2006.

[15] Richard L. Gustavsen, Russell J. Gehr, Scott M. Bucholtz, Robert R. Alcon, and Brian D. Bartram. Shock initiation of the tri-amino-tri-nitro-benzene based explosive PBX 9502 cooled to 55C. *Journal of Applied Physics*, 112(7):074909, 2012.

[16] R. L. Gustavsen, B. D. Bartram, L. L. Gibson, A. H. Pacheco, J. D. Jones, and A. B. Goodbody. Shock initiation of the TATB-based explosive PBX 9502 heated to 130C. *AIP Conference Proceedings*, 1979(1):100015, 2018.

[17] L G Hill, R L Gustavsen, R R Alcon, and S A Sheffield. Shock Initiation of New and Aged PBX 9501 Measured with Embedded Electromagnetic Particle Velocity Gauges. 9 Los Alamos National Laboratory, LA-13634-MS, 1999.

[18] Scott Jackson. The detonation cylinder test: Determination of full wall velocity and shape from a single velocimetry probe with an arbitrary angle. *AIP Conference Proceedings*, 1793(1):050017, 2017.